

## **A dynamic analysis of the underwriting cycle in non-life insurance**

Rocco Roberto Cerchiara<sup>1</sup>, Fabio Lamantia  
*Department of Business Science  
Faculty of Economics  
University of Calabria  
Italy*

### **Abstract**

The European Project Solvency II is devoted to the appraisal of a Solvency Capital Requirement that should capture the overall risk profile of insurance companies. In this framework there is a growing need to develop so-called internal risk models to get accurate estimates of liabilities. In the context of non-life insurance, it is crucial to correctly assess risk from different sources, such as underwriting risk with particular reference to premium, reserving and catastrophe risks. In particular the underwriting cycle is not quantified in standard formula under Quantitative Impact Study 4, but probably it could be included, as it provides additional volatility to liabilities distribution and so it could increase the capital requirement.

The aim of this paper is to correctly model the underwriting cycle for non-life insurance companies, also taking into account its effect on the solvency ratio. Starting from Collective Risk Theory, a dynamic control policy is defined to specify the relationship between solvency ratio and safety loading, to model the underwriting cycle. The corresponding dynamic equation for the solvency ratio, under some assumptions, assumes the form of a one dimensional *piecewise linear* map. In the first part of the work a deterministic version of this map is analyzed, where aggregate losses are simply regarded as a parameter. Numerical analysis and stochastic assessments of the model conclude the work.

*Key words:* non-life insurance, underwriting cycle, solvency ratio, collective risk theory, piecewise-linear dynamical systems, border collision bifurcations.

---

<sup>1</sup> Corresponding author, Fax +39-0984492277, cerchiara@unical.it

## 1. Introduction

The European Project Solvency II is devoted to the appraisal of a Solvency Capital Requirement that should capture the overall risk profile of insurance companies. In this framework there is a growing need to develop so-called internal risk models to get accurate estimates of liabilities. In the context of non-life insurance, it is crucial to correctly assess risk from different sources, such as underwriting risk with particular reference to premium, reserving and catastrophe risks. Technical specifications in Quantitative Impact Studies 4 (QIS4 – see CEIOPS, 2007), describe Underwriting Risk as: *the specific risk arising from insurance contracts. It relates to the uncertainty about results of the insurer's underwriting*. But QIS4 doesn't define any additional capital requirement for underwriting cycle. It is worth mentioning that *the underwriting cycle contributes an artificial volatility to underwriting results that lies outside the statistical realm of insurance risk* (Meyers, 2007). So for Internal Model development under Solvency II, underwriting cycle must be analyzed, because the additional volatility could produce a higher capital requirement.

Typically, in adverse development of financial positions, company's management tends to raise premium rates or reinsurance, whereas otherwise it increases dividends or reduces premium rates. A correct analysis of this phenomena is also significant to understand the evolution of the reserving cycle (that won't be considered in this paper), which is often correlated, with a lag period, with the underwriting cycle; in fact, it has been ascertained that insurers tend to over-estimate technical reserves during the hard part of the cycle, when loss ratios are low, and under-estimate these reserves in the opposite case (see for example Deloitte, 2008).

Feldblum (2001) discusses the causes of the underwriting cycle, taking into account insurance industry aspects (product differentiation, cost structures, barriers to entry, etc.) that could influence insurer solvency. The presence and length of cycles could depend on technical and non technical aspects such as position and competitiveness of leader companies in relation to the market, firm's tendency to increase its own market share; internal and external inflation of claim costs and change in premium rates, loyalty changes, exposition variations. The inability to obtain profits at the end of a cycle could produce reduction of market share and loss of business as well as a reduction in the solvency ratio.

There are several papers devoted to analyze and model underwriting cycle. It is worth mentioning the so-called financial pricing models (based on discounted cash flows). Originally Venezian (1985) and afterward Cummins and Outreville (1987), Haley (1995), Leng and Meier (2006) have used this approach, mainly based on time series analysis, to confirm the adoption of theories based on rational expectations and absence of financial market imperfections.

Another possible approach is given by capacity constraint models, based on the assumption that, in front of constraints deriving from regulatory capital requirement, the insurer has always an excess of capital, as to avoid the risk to demand capital externally; on this point see Gron (1994), Winter (1994), Choi et al. (2002), Higgins and Thistle (2000) and Derien (2008). In particular the two last papers proposed so called "regime switching" techniques, to eliminate the assumption of invariance of the model parameters in every phase of the cycle; in particular the last quoted paper discussed the exclusion of underwriting cycle in QIS4 standard formula. For further improvements in this kind of models, see also Cummins and Danzon (1997).

Other studies have been principally based on actuarial models, in particular the proposed approaches include:

- 1) Deterministic models (trigonometric functions), as considered in Daykin et al. (1994);
- 2) Time Series analysis (see Daykin et al., 1994, Cummins and Outreville, 1987);
- 3) Exogenous impacts: combined use of the previous ones, incorporating also external factors (for instance national economy trends or exposition) and simulation models, as shown in Pentilkainen et al. (1989) and Daykin et al. (1994). See also Sandstrom (2005) for a link with solvency II – standard formula approach proposed in QIS4.

In the next sections, an actuarial model will be employed in order to correctly model the underwriting cycle for non-life insurance companies, also taking into account the effect on the solvency ratio adopting an approach based on piecewise-linear dynamical systems, in order to investigate also the long-time horizon dynamic of the model (remember that QIS4 standard formula has been developed considering a one-year time horizon only). The basic model is derived from Collective Risk Theory. Besides a dynamic control policy (see Pentikainen et al., 1989 for a summary of the main control theory concepts), this permits to specify the relationship between solvency ratio and safety loading, in order to model the underwriting cycle. In particular a simplified formula of safety loading is derived that assumes the form of a one dimensional piecewise linear map, whose state variable is the solvency ratio.

The paper is organized as follows. In Section 2 an actuarial model under Collective Risk Theory is specified and its main dynamic properties are analyzed in section 3, including some brief considerations on the asymptotic properties of the solvency ratio. Section 4 collects some empirical results Section 5 concludes, also suggesting further improvements of the model.

## 2. Model specifications

The basic model is derived from Collective Risk Theory (see Daykin et al., 1994, Klugman et al., 1998 and Dhaene et al., 2001 for more details), where the solvency ratio  $u(t)$ , i.e. risk reserve  $U(t+1)$  on risk premium  $P(0)$ , at the end of the year  $t+1$  (not considering expenses and relative loadings) is given by:

$$u(t+1) = r u(t) + [1 + \lambda(t+1)]p(t+1) - x(t+1) \quad (1)$$

where

- $r$  is a function (constant for our purposes) of the rate of return  $j$ , the rate of portfolio growth  $g$  and the inflation rate  $i$  (supposed constants):  $r = \frac{1+j}{(1+g)(1+i)}$ ;
- $x(t+1)$  is the ratio of present value of aggregate loss  $X(t+1)$  on risk premium;
- $p(t+1)$  is the ratio of risk premium  $P(t+1) = E[x(t+1)]$  on initial level risk premium  $P(0) = E[X(0)]$ ;
- $\lambda(t+1)$  is the safety loading.

Starting from the idea of Daykin et al. (1994), in this paper a dynamic control policy is proposed to specify the relationship between solvency ratio and premium rates (underwriting cycle). For this reason, it is assumed the following dynamic equation for the safety loading:

$$\lambda(t+1) = \lambda_0 + c_1 \max[0, R_1 - u(t)] - c_2 \max[0, u(t) - R_2]. \quad (2)$$

where we assume that  $0 < R_1 \leq R_2$ . Equation (2) shows how, starting from a basic level  $\lambda_0$ , safety loading will be dynamically:

- increased, with a percentage of  $c_1$ , if  $u(t)$  decreases under a floor level  $R_1$  or
- decreased, with a percentage of  $c_2$ , if  $u(t)$  is higher than a roof level  $R_2$ .

Note that  $c_1$ ,  $c_2$ ,  $R_1$ ,  $R_2$  could represent strategic parameters which depend on risk management choices.

Under the rough assumption that aggregate loss distribution doesn't change in time, so that  $p(t+1) = p(t) = p(t-1) = \dots = 1$  (not considering also time lag effects), we define a simplified version of (1) that assumes the form of a one dimensional *piecewise linear* map in the state variable  $u(t)$ :

$$u(t+1) = r u(t) + \{1 + \lambda_0 + c_1 \max[0, R_1 - u(t)] - c_2 \max[0, u(t) - R_2]\} - x(t+1) \quad (3)$$

This dynamic control obviously prevents the tendency to infinity of  $u(t)$ , which is the typical situation on long-term process for  $r \geq 1$ . In this paper we generalize the proof of Daikin et al. (1994) for asymptotic behaviour of  $u(t)$  in a long-term process, introducing this dynamic control policy thus obtaining different levels of equilibrium, varying in particular the parameter  $r$ . In doing so, we don't use, at least in a simplified setting, any simulation approach, but only analytical results on piecewise-linear dynamical systems.

In next section, it is analyzed a deterministic version of this map, where  $x(t+1)=x$  is simply regarded as a parameter. In this case local and global analysis of (3) can be analytically performed, showing the long-term behaviour of the solvency ratio  $u(t)$  as the main parameters of the model vary. In particular we detect so called "Border-collision bifurcations" (see Di Bernardo et al., 2008 for details), related to the crossing of the trajectory of (3) into regions where the definition of the map changes. An example of stochastic assessments of (3) conclude the work in section 4.

### 3. Deterministic solving ratio dynamic: equilibrium analysis and bifurcations

In this paragraph we describe the deterministic dynamic of the solvency ratio  $u(t)$  as specified by equation (3) with  $x(t+1)=x$ . We first observe that (3) can be also described as

$$u(t+1) = f(u(t)) = r u(t) + 1 + \lambda_0 - x + \begin{cases} c_1(R_1 - u(t)) & \text{if } u(t) < R_1 \\ 0 & \text{if } R_1 \leq u(t) \leq R_2 \\ c_2(R_2 - u(t)) & \text{if } u(t) > R_2 \end{cases} \quad (4)$$

Where, of course,  $c_1, c_2 \in [0, 1]$ . Without enforcing any control it is  $c_1 = c_2 = 0$ , and dynamical system (4) reduces to a linear map, whose unique equilibrium<sup>2</sup>  $u_M^* = \frac{1 + \lambda_0 - x}{1 - r}$  (provided  $r \neq 1$ ) is globally asymptotically stable as long as  $r < 1$  and unstable otherwise.

In the general case, map (4) is piecewise linear, since it is continuous at each point and there is an interval partition of the domain where the map is linear in each interval; however it presents (up to) two kinks at the points  $u_1 = R_1$  and  $u_2 = R_2$ , where the definition of the map changes. Moreover we observe that if  $r > \max[c_1, c_2]$  then (4) is strictly increasing.

Different expression of fixed points are obtained according to the branch of the map  $f(\cdot)$  that intersects the identity map. Since there are basically three different branches for (4) we can have the following possible equilibria:

$$u_L^* = \frac{1 + \lambda_0 + c_1 R_1 - x}{1 - r + c_1}; \quad u_M^* = \frac{1 + \lambda_0 - x}{1 - r}; \quad u_H^* = \frac{1 + \lambda_0 + c_2 R_2 - x}{1 - r + c_2} \quad (5)$$

<sup>2</sup> We recall that an equilibrium (or steady state or fixed point)  $u^*$  of a unidimensional map, such as (4), is a solution of the algebraic equation  $u^* = f(u^*)$ .

The number of equilibria and their dynamic property depends on the parameter configuration, as we show below. The following proposition holds.

**Proposition.** *Assume that  $0 < r < 1$ . Then the dynamical system (4) has a unique equilibrium  $u^*$ , which is globally asymptotically stable.*

**Proof.** Under the hypothesis that  $0 < r < 1$  we have that  $\frac{|f(u(t+1)) - f(u(t))|}{|u(t+1) - u(t)|} < 1$  so the map  $u(t+1)=f(u(t))$  specified in (4) is a contraction. Hence the fixed point  $u^*$  is unique and globally asymptotically stable. Moreover it is straightforward to show that if  $R_2 \geq R_1 > \frac{1+\lambda_0-x}{1-r}$  then this unique equilibrium is indeed  $u_L^*$ ; otherwise if  $R_1 \leq \frac{1+\lambda_0-x}{1-r} \leq R_2$  then it is  $u_M^*$  and finally the fixed point is  $u_H^*$  if  $\frac{1+\lambda_0-x}{1-r} > R_2 \geq R_1$  holds. As pointed out before, condition  $r > \max[c_1, c_2]$  ensures that (4) is strictly increasing so that the convergence to the fixed point is always monotonic. Otherwise we can observe convergence with damped oscillations around the unique equilibrium. QED

As for the case  $r > 1$ , we already established that (4) is in this case a strictly increasing map. If no equilibrium exists, then the generic trajectory of  $u(t)$  will diverge to infinity.

If  $R_1 > -\frac{1+\lambda_0-x}{c_1}$ , then the level  $u_L^* = \frac{1+\lambda_0+c_1R_1-x}{1-r+c_1}$  is an equilibrium for (4) if and only if it is also  $\frac{1+\lambda_0-x}{1-r} > R_1$ . In addition,  $u_L^*$  is always stable in this case, since it must be  $f'(u_L^*)=r-c_1 < 1$  to ensure that  $u_L^*$  is indeed an equilibrium.

Otherwise for  $R_1 < -\frac{1+\lambda_0-x}{c_1}$ ,  $u_L^*$  is an equilibrium for (4) if and only if condition  $\frac{1+\lambda_0-x}{1-r} < R_1$  holds. In symmetry with the previous case, now  $u_L^*$  cannot be stable since it must necessarily be  $f'(u_L^*)=r-c_1 > 1$ . In the border case  $R_1 = -\frac{1+\lambda_0-x}{c_1}$  we have that  $u_L^* = 0$  is an equilibrium.

In general  $u_M^*$  is a fixed point if and only if it is  $R_1 \leq \frac{1+\lambda_0-x}{1-r} \leq R_2$  and it is always unstable since  $f'(u_M^*)=r > 1$ .

The study of  $u_H^* = \frac{1+\lambda_0+c_2R_2-x}{1-r+c_2}$  is similar to the one carried out for  $u_L^*$ . In fact when  $\frac{1+\lambda_0-x}{1-r} < R_2$  and  $r-c_2 < 1$  then the equilibrium  $u_H^*$  exists and it is locally stable. Otherwise for  $\frac{1+\lambda_0-x}{1-r} > R_2$  and  $r-c_2 > 1$  then  $u_H^*$  is an equilibrium but it is unstable in this case. The generic trajectory not starting in  $u_H^*$  either diverges or converges to  $u_L^*$  (provided it exists).

Finally when  $R_1 = \frac{1+\lambda_0-x}{1-r}$  (and/or  $R_2 = \frac{1+\lambda_0-x}{1-r}$ ) it is  $u_L^* = u_M^*$  (respectively  $u_H^* = u_M^*$ ), which is always unstable.

We remark that, when  $r > 1$ , all three fixed points previously specified can exist simultaneously. A necessary and sufficient condition for this to happen is that

$$R_2 > \frac{1 + \lambda_0 - x}{1 - r} > R_1 > -\frac{1 + \lambda_0 - x}{c_1} \quad \text{and } r - c_2 < 1$$

In this case  $u_L^*$ ,  $u_M^*$  and  $u_H^*$  are indeed (distinct) equilibria, and as we have shown previously, both  $u_L^*$  and  $u_H^*$  are locally asymptotically stable, as map (4) must necessarily have there slope  $0 < s < 1$ . Since, in this case, map (4) is strictly increasing and  $u_L^*$  and  $u_H^*$  are locally asymptotically stable, we have that for any initial condition  $u(0) \in (-\infty, u_M^*) = B(u_L^*)$  it is  $\lim_{n \rightarrow \infty} f^n(u(0)) = u_L^*$ , whereas for an i.c.  $u(0) \in (u_M^*, +\infty) = B(u_H^*)$  we have that  $\lim_{n \rightarrow \infty} f^n(u(0)) = u_H^*$ <sup>3</sup>. In the dynamical system jargon,  $B(u_L^*)$  and  $B(u_H^*)$  are called the “basin of attraction” of fixed points  $u_L^*$  and  $u_H^*$ . The case  $r = 1$  can be studied similarly. We remark that in this case when  $1 + \lambda_0 - x = 0$  all  $u \in [R_1, R_2]$  consist of fixed points.

Up to this point we considered the basic configuration of fixed points for a given set of parameters. As the main parameters vary we can observe a change in the type of fixed point and/or their stability properties.

For simplicity we begin by considering the case  $1 + \lambda_0 - x = 0$  and the parameter  $r < 1$ :  $u_L^*$  is now the unique stable equilibrium, since the condition for its existence and stability reduces to  $R_2 \geq R_1 > 0$ , which holds true. If we let  $r$  increase but maintaining  $r < 1$ , we only observe an increase in the  $u_L^*$  value, that remains asymptotically stable: the generic trajectory converges exactly to  $u_L^*$ . At  $r = 1$  a bifurcation occurs and all  $u \in [R_1, R_2]$  are fixed points. For  $1 < r < 1 + c_2$  we have that now  $u_H^*$  is the stable equilibrium. If draw a bifurcation diagram in the plane  $(r, u)$ , i.e. we plot the asymptotic value for the solvency ratio  $u$  for a given  $r$ , we observe that as long as  $r < 1$  the asymptotic value  $u_L^*$  continuously increases as  $r$  increases. However at  $r = 1$  a jump discontinuity on the bifurcation diagram occurs at which the asymptotic state abruptly goes from  $u_L^*$  to  $u_H^*$ . This can be restated by saying that as  $r$  crosses the bifurcation value 1, a “small variation” of  $r$  leads to a “large variation” on the solvency ratio equilibrium value.

The previous example introduces us to a more general situation, which can be observed in the model (4) for a wider selection of the main parameters.

Let us consider again the case where 1)  $\frac{1 + \lambda_0 - x}{1 - r} < R_2$ , with  $1 < r < 1 + c_2$  and 2)

$$R_1 > \max \left[ -\frac{1 + \lambda_0 - x}{c_1}, \frac{1 + \lambda_0 - x}{1 - r} \right].$$

Condition 1) implies that  $u_H^*$  exists and it is locally stable

whereas condition 2) implies that both  $u_L^*$  and  $u_M^*$  are not steady states.

As the parameter  $\lambda_0$  is decreased (or equivalently  $x$  is increased) such that  $R_1 = \frac{1 + \lambda_0 - x}{1 - r}$ , a *fold*

bifurcation occurs at which the fixed point  $u_M^*$  is created. For further decreasing of  $\lambda_0$  (or  $-x$ ), all three steady states exists. However if we further decrement  $\lambda_0$  (or  $-x$ ) up to the level

$$R_2 = \frac{1 + \lambda_0 - x}{1 - r}$$

a second fold bifurcation occurs at which  $u_M^*$  and  $u_H^*$  merge and disappear.

<sup>3</sup> Here  $f^n$  denotes the  $n$ -th iterate of the map, i.e. the composition of  $f$  with itself  $n$  times.

Hence for an initial condition sufficiently close to  $u_H^*$  we can observe also in this case a jump discontinuity in the bifurcation diagram as  $\lambda_0$  (or  $-x$ ) decreases. In fact when  $u_H^*$  is the only attractor of the model, the generic trajectory converges to it. As  $u_L^*$  and  $u_M^*$  are created, the generic trajectory sufficiently close to  $u_H^*$  still converges to this attractor. However, at the second bifurcation  $u_H^*$  disappears so that the generic trajectory now converges to the unique attractor,  $u_L^*$  (provided it is also  $r < 1 + c_I$ ). This double fold bifurcation is indeed the cause of the jump discontinuity in the bifurcation diagram as parameter  $\lambda_0$  (or  $x$ ) varies.

We remark that, even if the fold bifurcation is a well known phenomenon in the context of “smooth“ unidimensional maps, here in map (4) we have a so called “border collision” bifurcations. In fact, in map (4) fold bifurcations cannot be detected by the usual condition that the eigenvalue at the fixed point is equal to one. Indeed (4) is not differentiable at the bifurcation point. However a “fold” border collision bifurcation occurs as a fixed point collides with the border where the definition of the map changes and the map is not differentiable there.

#### 4. Numerical results

In this section we show numerically the main dynamic scenarios that can be generated by model (3) for certain parameter constellations. We remark that all numerical results of this section have an analytical justification, as given in section 3. For this purpose, we carry on a unifying example, exploring it from different viewpoints firstly in a deterministic setting and then in a stochastic framework.

Let us consider the case depicted in figure 1, where the map (3) is represented in the space  $u(t)$  and  $u(t+1)$  for different values of  $r$ . This kind of representation is useful, as an equilibrium point can be graphically identified as an intersection point between the graph of the map (3) with a 45° degree line.

In particular we fix the model parameters as  $c_1=0.632$ ;  $c_2=0.754$ ;  $R_1=1.91$ ;  $R_2=4.43$ ;  $x=4.5$ ;  $\lambda_0=2.79$  and we let  $r$  vary, passing from values below 1 to values above 1.

In Figure 1(a), where  $r=0.98$ , a unique equilibrium point  $u_L^*$  exists and it is globally asymptotically stable; hence any trajectory, regardless to its initial conditions, will eventually converge to  $u_L^*$ , which is the long run outcome of the system. As  $r$  crosses the value 1, the dynamic behaviour of the map can be very different from what is obtained with  $r$  less than one. In fact, at  $r=1.16$  a branch of the map meet the 45° degree line and so it is created a new equilibrium point, which coexists with  $u_L^*$  [see Figure 1(b) just at the bifurcation value]. As previously discussed, this change of the dynamic behaviour represents a bifurcation, that for this particular map always occurs in points of nondifferentiability.

As  $r$  is further increased, all three equilibria  $u_L^*$ ,  $u_M^*$  and  $u_H^*$  are present at the same time, as shown in Figure 1(c), where  $r=1.2$ . In this case, however, only equilibria  $u_L^*$  and  $u_H^*$  are locally stable, i.e. only trajectories whose initial conditions are sufficiently close to these equilibria will eventually converge to these points. In particular the equilibria  $u_M^*$  is a watershed that separate the basin of attraction of the stable equilibria  $u_L^*$  and  $u_H^*$ , as already described in section 3. However as  $r$  is increased further, equilibria  $u_L^*$  and  $u_M^*$  merge and disappear, through a bifurcation similar to the previous one; afterward only the stable equilibrium  $u_H^*$  exists. In figure 1(d) it is represented such a case after this last bifurcation has taken place, with  $r=1.44$ .

We can summarize this result by observing that a double “border collision” bifurcation occurs, for increasing values of  $r$ , so that the attractor of the system passes from a value with a “low”  $u$  to another one with an higher value, with an intermediate phase characterized by coexistence of attractors.

This result is very interesting from a comparative dynamic point of view. In fact, let us consider what happens before the first bifurcation. As the only globally stable attractor is  $u_L^*$ , we know that a generic trajectory is forced to converge to this attractor. Locally we still observe convergence to  $u_L^*$  even after the first bifurcation took place (i.e. for values of  $r > 1.16$ ), as  $u_L^*$  is an attractor for all trajectories starting below  $u_M^*$ . However, after the second bifurcation, the only stable attractor is  $u_H^*$ , so that a generic attractor is forced to jump to this equilibrium and to converge to it in the long run.

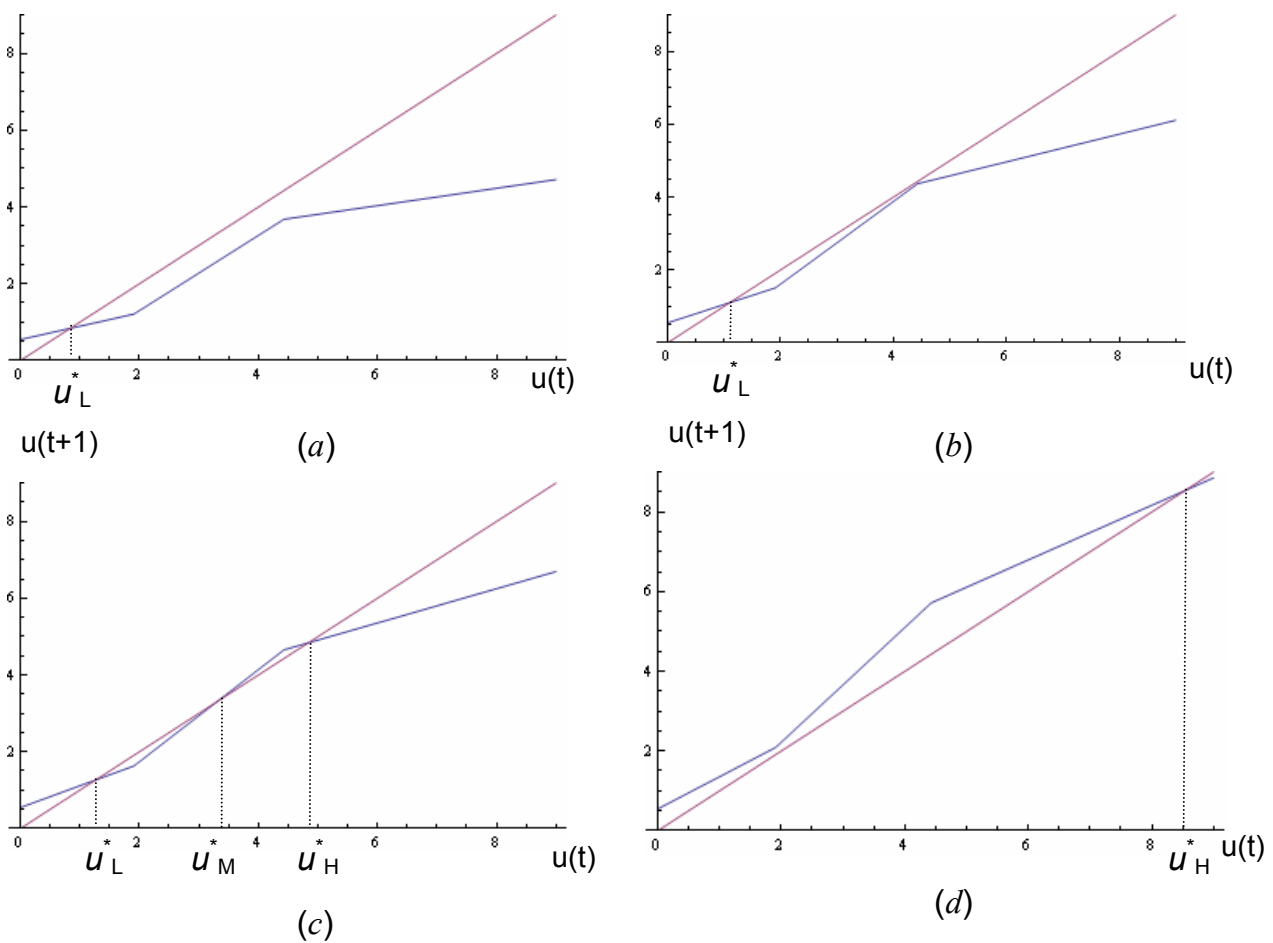


**Figure 1.** Double “border collision” bifurcation for increasing  $r$ .

In Figure 2 we present what it is called a bifurcation diagram, i.e. a representation of the possible long-term values (equilibria, periodic points, etc.) of the system as a function of a bifurcation parameter. In particular in figure 2 (a) and (b) the long run evolutions of the safety loading  $\lambda(n)$  and the solvency ratio  $u(n)$  are respectively depicted, i.e. the limit of these quantities, generated by equations (2) and (3), as  $n$  goes to infinity. For this particular case we let vary the basic level of the safety loading  $\lambda_0$  (from 2.36 to 3.55), and we keep all other parameters as in Figure 1 and with  $r=1.20$ . The long run safety level converges to an equilibrium, which is increasing and continuous in  $\lambda_0$  [see figure 2(a)], whereas the bifurcation diagram for the long run solvency ratio, though

increasing in  $\lambda_0$ , presents a jump discontinuity, whose formation is due to the change of the stable attractor after the second bifurcation takes place.

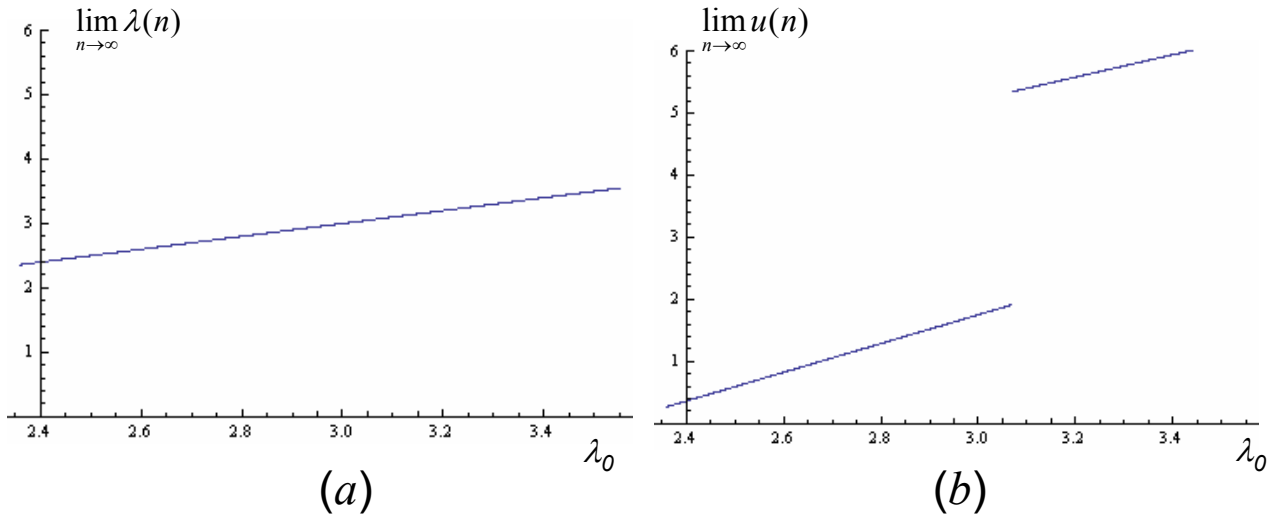


**Figure 2.** Double “border collision bifurcation” for increasing  $\lambda_0$  and its effects on the long run equilibrium value of the solvency ratio.

Up to this point we regarded the aggregate loss  $x$  as a constant parameter. Now we try to ascertain how the presence of a stochastic aggregate loss can influence the long-run evolution of the solvency ratio. In figure 3 we fixed the parameters  $c_1, c_2, R_1, R_2$  as in the previous examples, with a basic safety loading  $\lambda_0=2.79$ . In this stochastic assessment we considered an aggregate loss defined by  $x = 4.5z$ , where  $z$  is distributed according to a Lognormal with  $\mu=0$  and  $\sigma=0.05$ . Starting from the same initial condition, we simulated 200 independent trajectories and we plotted an asymptotic value for  $u(n)$ , with  $n=500.000$ . In figure 3(a), where  $r < 1$  (it is precisely  $r = 0.92$ ), we observe a small displacement between each trajectory’s long run level and a mean equilibrium level (depicted as the horizontal line), which is the long run level in the deterministic setting. Formally a mean equilibrium level is obtained by substituting the mean value of the aggregate loss in (5). On the other hand, the picture can change radically when  $r > 1$ . In figure 3(b), where  $r=1.2$ , two attractors coexists and most trajectories stay close to the low mean equilibrium level, as their identical initial conditions are close to it. However it is possible, as a consequence of the stochastic aggregate loss, that some trajectories enter the basin of attraction of the higher mean equilibrium level, thus approaching it in the long run (see the higher horizontal line). As a results an higher volatility of the state variable is observed, as clearly shown by the peaks in figure 3(b).

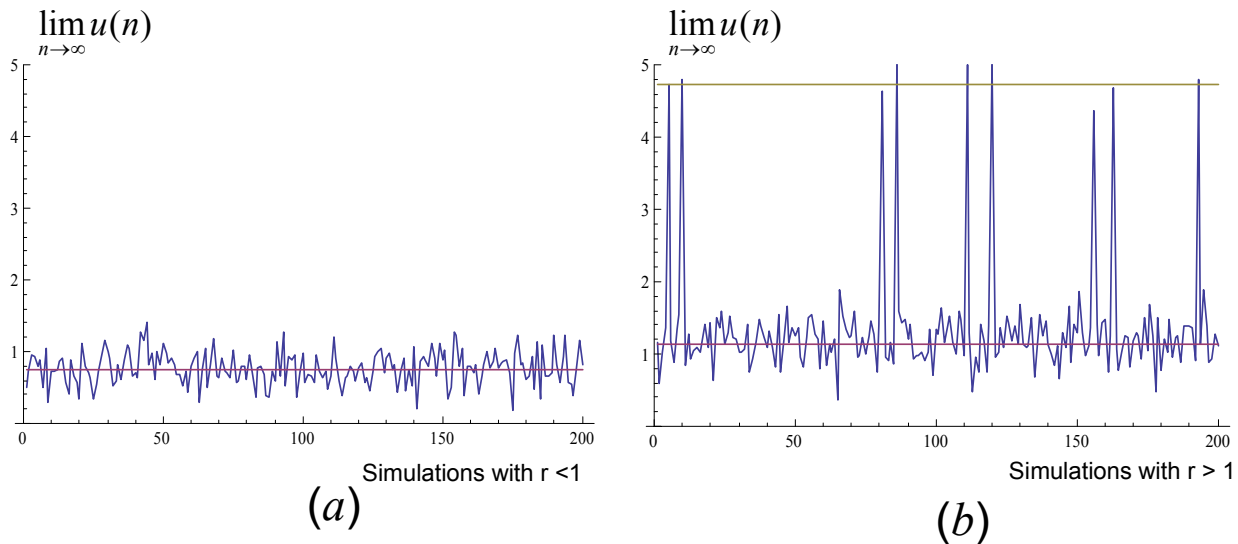


Figure 3. Trajectory with 200 independent simulations.

Logically the results of this particular example depend on the adopted parameter values and on initial condition of the system. However this example shows that the theory of piecewise linear dynamical systems together with simulations can turn out to be very useful for assessments within the Solvency 2 framework, where often different approaches are necessary for a better understanding and quantification of particular risks, especially for underwriting risk of non-life insurance companies.

## 5. Concluding Remarks

In this paper we generalized the proof in Daikin et al. (1994) of the asymptotic behaviour of solvency ratio  $u(t)$ , when a dynamic control policy is introduced. In particular different equilibrium levels and analytical conditions for their coexistence can be obtained.

Within the proposed model, it is possible to define analytical control rules by setting the strategic parameters  $c_1, c_2, R_1, R_2$  and, consequently, to dynamically update the safety loading level. With this approach it is possible to “guarantee” prefixed equilibrium levels of the solvency ratio and so of the insurer’s capital requirements. We showed, both analytically and numerically, the dynamic behaviour that can be generated by the underlying model, and in particular the possibility of sudden jumps in the solvency ratio, technically as a consequence of a double “border collision” fold bifurcation.

All in all we think that this method could be very useful for internal models developments under Solvency 2. In fact this approach could represent an alternative (or a complementary) tool to the traditional techniques employed in actuarial application, such as standard simulations, approximation formulas, etc.

This paper represents only a first step toward the use of these techniques and will be extended in subsequent works. In fact we are working on further developments, such as testing other dynamic control policies, estimating probability distributions when bifurcations of the underlying map occur and assessing, with real insurance data, aggregate losses and parameters estimations for stochastic implementations.

## Acknowledgements

We acknowledge comments from the participants at the *Actuarial and Financial Mathematics Conference*, Bruxelles February 2009. The first author benefited from the research project “Models for evaluation of insurance risk”, MIUR, Italy. The usual disclaimer applies.

## References

- [1] CEIOPS (2007). Quantitative Impact Studies 4 - Technical Specifications. <http://www.ceiops.eu/content/view/118/124/>
- [2] Choi, S., Hardigree, D. and Thistle, P. (2002). The property-liability insurance cycle: A comparison of alternative models. *Southern Economic Journal*, **68**, 530–548.
- [3] Cummins, J.D. and Outreville, J.F. (1987). An international analysis of underwriting cycle. *Journal of Risk and Insurance*, **54**, 246–262.
- [4] Cummins, J.D. and Danzon, P. (1997). Price, Financial Quality and Capital Flows in Insurance Markets. *Journal of Financial Intermediation*, **6**, 3–38.
- [5] Daykin, C. D., Pentikainen, T. and Pesonen, M. (1994). Practical Risk Theory for Actuaries. London: Chapman and Hall.
- [6] Deloitte (2008). Reserving through the softening market. *Faculty of Actuaries Student Society, Current Topics, General Insurance*.
- [7] Derien, A. (2008). An Empirical Investigation of the Factors of the Underwriting Cycles in Non-Life Market. *Proceedings of International Conference MAF*.
- [8] Dhaene, J., Denuit, M., Goovaerts, M.J. and Kaas, R. (2001). Modern Actuarial Risk Theory. Dordrecht: Kluwer Academic Publishers.
- [9] Di Bernardo, M, Budd, C.J., Champneys, A.R. and Kowalczyk, P. (2008). Piecewise-smooth dynamical systems. London: Springer Verlag.
- [10] Feldblum, S. (2001), Underwriting cycles and business strategies. *Proceedings of the Casualty Actuarial Society*, **58**, 175-235.
- [11] Gron, A. (1994). Evidence of capacity constraint and cycle in insurance markets. *Journal of Law and Economics*, 37.
- [12] Haley, J.D. (1995). A by line cointegration analysis of underwriting margins and interest rates in the property-liability insurance industry. *Journal of Risk and Insurance*, 62, 755–763.
- [13] Higgins, M. and Thistle, P. (2000). Capacity constraints and the dynamics of underwriting profits. *Economic Inquiry*, **38**, 442–457.
- [14] Klugman, S., Panjer, H. and Willmot, G. (1998). Loss Models - From Data to Decisions. New York: John Wiley & Sons. First Edition.
- [15] Leng, C. and Meier, U. (2006). Analysis of multi national underwriting cycles in property liability insurance. *The Journal of Risk Finance*, **7**, 146–159.
- [16] Meyers, G. (2007). The common shock model for correlated insurance losses. *Variance*, **1**, Issue 1, 40-52.

- [17] Pentikainen, T., Bondsdorff, H., Pesonen, M., Rantala, J. and Ruohonen, M. (1989). Insurance solvency and financial strength. Helsinki: *Finnish Insurance Training and Publishing Company Ltd.*
- [18] Sandstrom, A. (2005). Solvency – Models, Assessment and Regulation. London: Chapman and Hall.
- [19] Venezian, E. (1985). Ratemaking method and profit cycles in property and liability insurance. *Journal of Risk and Insurance*, **52**, 477-500.
- [20] Winter, R. (1994). The dynamics of competitive insurance markets. *Journal of Financial Intermediation*, **3**, 379–415.